

# REPORT DOCUMENTATION PAGE

Form Approved  
OMB No. 0704-0188

Public reporting burden for this collection of information is estimated to average 1 hour per response, including the time for reviewing instructions, searching existing data sources, gathering and maintaining the data needed, and completing and reviewing this collection of information. Send comments regarding this burden estimate or any other aspect of this collection of information, including suggestions for reducing this burden to Department of Defense, Washington Headquarters Services, Directorate for Information Operations and Reports (0704-0188), 1215 Jefferson Davis Highway, Suite 1204, Arlington, VA 22202-4302. Respondents should be aware that notwithstanding any other provision of law, no person shall be subject to any penalty for failing to comply with a collection of information if it does not display a currently valid OMB control number. **PLEASE DO NOT RETURN YOUR FORM TO THE ABOVE ADDRESS.**

<b>1. REPORT DATE (DD-MM-YYYY)</b> 01-05-2006		<b>2. REPORT TYPE</b> Conference Paper POSTPRINT		<b>3. DATES COVERED (From - To)</b> 2005 - 2006	
<b>4. TITLE AND SUBTITLE</b> Development of Concentrated Strain Based Deployable Truss Structures				<b>5a. CONTRACT NUMBER</b> FA9453-05-C-0005	
				<b>5b. GRANT NUMBER</b>	
				<b>5c. PROGRAM ELEMENT NUMBER</b> 63401F	
<b>6. AUTHOR(S)</b> Eric L. Pollard, Thomas W. Murphey,* Juan M. Mejia-Ariza†				<b>5d. PROJECT NUMBER</b> 682J	
				<b>5e. TASK NUMBER</b> SY	
				<b>5f. WORK UNIT NUMBER</b> 0A	
<b>7. PERFORMING ORGANIZATION NAME(S) AND ADDRESS(ES)</b> CSA Engineering, Inc. 1451 Innovation Pkwy SE, Suite 100 Albuquerque, NM 87123-3831				<b>8. PERFORMING ORGANIZATION REPORT NUMBER</b>	
<b>9. SPONSORING / MONITORING AGENCY NAME(S) AND ADDRESS(ES)</b> *Air Force Research Laboratory Space Vehicles 3550 Aberdeen Ave SE Kirtland AFB, NM 87117-5776				<b>10. SPONSOR/MONITOR'S ACRONYM(S)</b>	
				<b>11. SPONSOR/MONITOR'S REPORT NUMBER(S)</b> AFRL-VS-PS-TP-2006-1020	
<b>12. DISTRIBUTION / AVAILABILITY STATEMENT</b> Approved for public release; distribution is unlimited. (Clearance #VS06-0104)					
<b>13. SUPPLEMENTARY NOTES</b> Published in the 47 <sup>th</sup> AIAA/ASME/ASCE/AHS/ASC Structures, Structural Dynamics, and Materials Conference Proceedings, 1 - 4 May 2006, Newport, RI, AIAA 2006-1682.  Government Purpose Rights					
<b>14. ABSTRACT</b> The objective of this research is to develop a novel, deployable hierarchical truss architecture composed of extruded carbon fiber reinforced plastic (CFRP) rod and shape memory alloy (SMA) flexure elements; this structural system is representative of a concentrated, material deformation based deployable architecture. The scope of this study encompasses applying fundamental principles of rational truss design, relevant to all deployable structures, first to prove the concept at the individual element level, then to design the packaging kinematics, and finally, evaluate and scale the global performance of the system. Aspects of the architecture for tackle to further develop the truss concept, including manufacturing technology, experimental analysis, and the deployment scheme, will be reported in manuscripts to appear. Technology addressed through this research is intended to foster and mature successive large, launch-packaged concentrated strain structures.					
<b>15. SUBJECT TERMS</b> Truss Architecture, Carbon Fiber Reinforced Plastic, CFRP, SMA, Deployable Architecture					
<b>16. SECURITY CLASSIFICATION OF:</b>			<b>17. LIMITATION OF ABSTRACT</b> Unlimited	<b>18. NUMBER OF PAGES</b> 14	<b>19a. NAME OF RESPONSIBLE PERSON</b> Thomas W. Murphey
<b>a. REPORT</b> Unclassified	<b>b. ABSTRACT</b> Unclassified	<b>c. THIS PAGE</b> Unclassified			<b>19b. TELEPHONE NUMBER (include area code)</b> 505-846-9969

# Development of Concentrated Strain Based Deployable Truss Structures

Eric L Pollard\*

*CSA Engineering, Inc., Albuquerque, NM 87123-3831 US*

Thomas W Murphey†

*Air Force Research Laboratory, Albuquerque, NM 87117-5776 US*

&

Juan M Mejia-Ariza‡

*Virginia Polytechnic Institute & State University, Blacksburg, VA 24061-0344 US*

The objective of this research is to develop a novel, deployable hierarchical truss architecture composed of extruded carbon fiber reinforced plastic (CFRP) rod and shape memory alloy (SMA) flexure elements; this structural system is representative of a concentrated, material deformation based deployable architecture. The scope of this study encompasses applying fundamental principles of rational truss design, relevant to all deployable structures, first to prove the concept at the individual element level, then to design the packaging kinematics, and finally, evaluate and scale the global performance of the system. Aspects of the architecture for tackle to further develop the truss concept, including manufacturing technology, experimental analysis, and the deployment scheme, will be reported in manuscripts to appear. Technology addressed through this research is intended to foster and mature successive large, launch-packaged concentrated strain structures.

## Nomenclature

$A$	=	area
$b$	=	width
$d$	=	diameter
$D$	=	flexural rigidity
$E$	=	modulus of elasticity
$G$	=	shear modulus of elasticity
$h$	=	thickness
$I$	=	area moment of inertia
$J$	=	polar area moment of inertia
$l$	=	element length
$M$	=	critical moment
$v$	=	areal mass
$w$	=	linear mass
$\nu$	=	Poisson's ratio
$\rho$	=	mass density

---

\* Engineer, CSA Engineering, Inc., 1451 Innovation Pkwy. SE Suite 100, Albuquerque, NM 87123-3831 US, AIAA Young Professional Member

† Research Aerospace Engineer, Space Vehicles Directorate, 3550 Aberdeen Ave. SE, Albuquerque, NM 87117-5776 US, AIAA Professional Member

‡ Graduate Student, Macromolecular Science & Engineering Program, 2018 Hahn Hall, Blacksburg, VA 24061-0344 US

$f$  = flexure  
 $p$  = photopolymer  
 $r$  = rod

## I. Introduction

**D**EPLOYABLE, monolithic composite trusses historically require members to comply to a packaged configuration, compromising stiffness and incurring mass penalties for strength to accommodate reduced volume states.<sup>1</sup> Non-mechanically, collapsible architectures synthesized of piece-wise constant cross-section elements composed of structurally efficient, high-stiffness composite for the majority of their length and a less structurally efficient compliant material at either end of the span can maintain strength-stability and stiffness properties reasonably equivalent to a uniform high-stiffness composite element and yield an articulating structure relevant to deployable space applications. The notion of varying the stiffness along the length of a column has been argued to enable greater buckling resistance to mass efficiency than a simply supported uniform column.<sup>2</sup> This philosophy leads to monolithic systems packaged through concentrated, material deformation of flexure elements which have no dead-band and can exploit stored strain energy to motivate self-deployment. Shape memory alloy (SMA), capable of superelasticity, feature additions have been found to serve well as a compliant flexure material. Since discovery, superelasticity, a recoverable, solid-phase dependent inelastic deformation mechanism, has been identified as a potential agency to drive active material systems.<sup>3</sup> SMAs are particularly attractive for space applications due to their ability to recover large deformations by generating high specific force; these are resulting artifacts of the mechanically induced austenite-martensite crystalline phase transformation. Deployment and in-service challenges of large, launch-packaged space vehicle programs is expected to showcase the leverage SMA articulated, high-stiffness composite technology extends to structural reconfiguration and performance tailoring.

### A. Concept

This truss concept is a novel, deployable hierarchical architecture composed of extruded carbon fiber reinforced plastic (CFRP) rod and SMA flexure elements. The composite longerons and battens are joined via SMA flexures with unique joints to enable the Nitinol features to each flex about a single axis; the joints dictate the flexure bend radius and consequently the strain realized. In order to minimize the bend radius for increased compaction efficiency, a less structurally efficient material system is utilized for the hinge regions while a more efficient and less compliant material system is utilized throughout the majority of the structure. It may not be intuitive this pairing of structural roles leads to greater mass efficiency as well. One-order greater in hierarchy these elements form four-longeron trusses junctioning at hub boxes to serve as members in a one-dimensional truss network or formatted in two-dimensions, resulting in a grillage; the former variant is particularly suited for precision, kilometer-scale booms and the latter shallow structural format would serve as a non-precision system, such as a photovoltaic array or radar platform (Fig. 1).

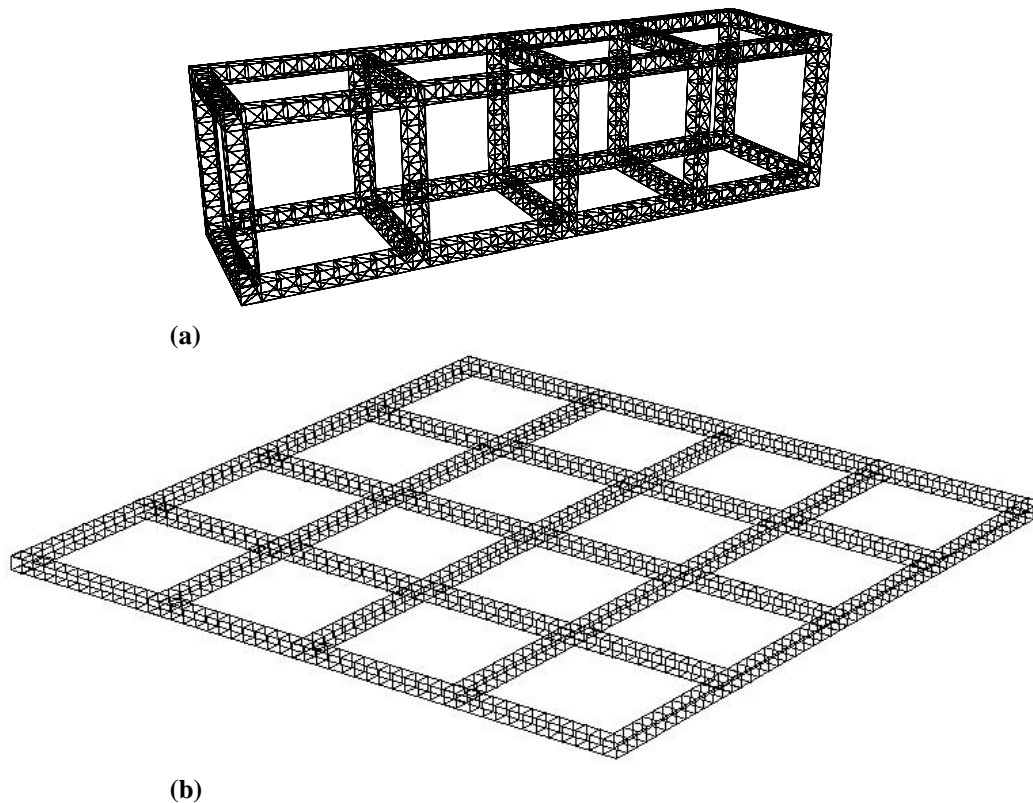


**Fig. 1 One-order greater in hierarchy these elements form four-longeron trusses junctioning at hub boxes to serve as members, (a) in a one-dimensional truss network; (b) or formatted in two-dimensions, resulting in a grillage.**

The hinge axes are deliberately oriented to enforce the kinematics, simultaneously shearing several truss bays in one direction to collapse the length with an increase in height followed by shearing of the hub boxes twice. The first packaging stage is similar to the movement of the Pactruss design as described in Refs. 4-6. Example modeled assemblies of the truss concept depict the system at each stage of the sequence: two-, deployed trusses terminating at three-, deployed hub boxes, simultaneously sheared truss bays to collapse these assemblies against faces of the hub boxes, the first hub box shear and the second shear of the left truss as one event, and the last stage, the second hub box shear and the second shear of the right truss as one event. Note the truss batten frames are not included in this sequence (Fig. 2). With some creativity, one can extrapolate how this pattern propagates through the two-dimensional format; this kinematic design is also valid for the boom variant where the movement of the two grillages forming opposite faces of the truss would mimic the two-dimensional sequence and the batten elements connecting these two faces would participate in the final two-stages. Linear compaction ratios of 400:1 and volumetric compaction ratios of 2,000:1 are reasonable.

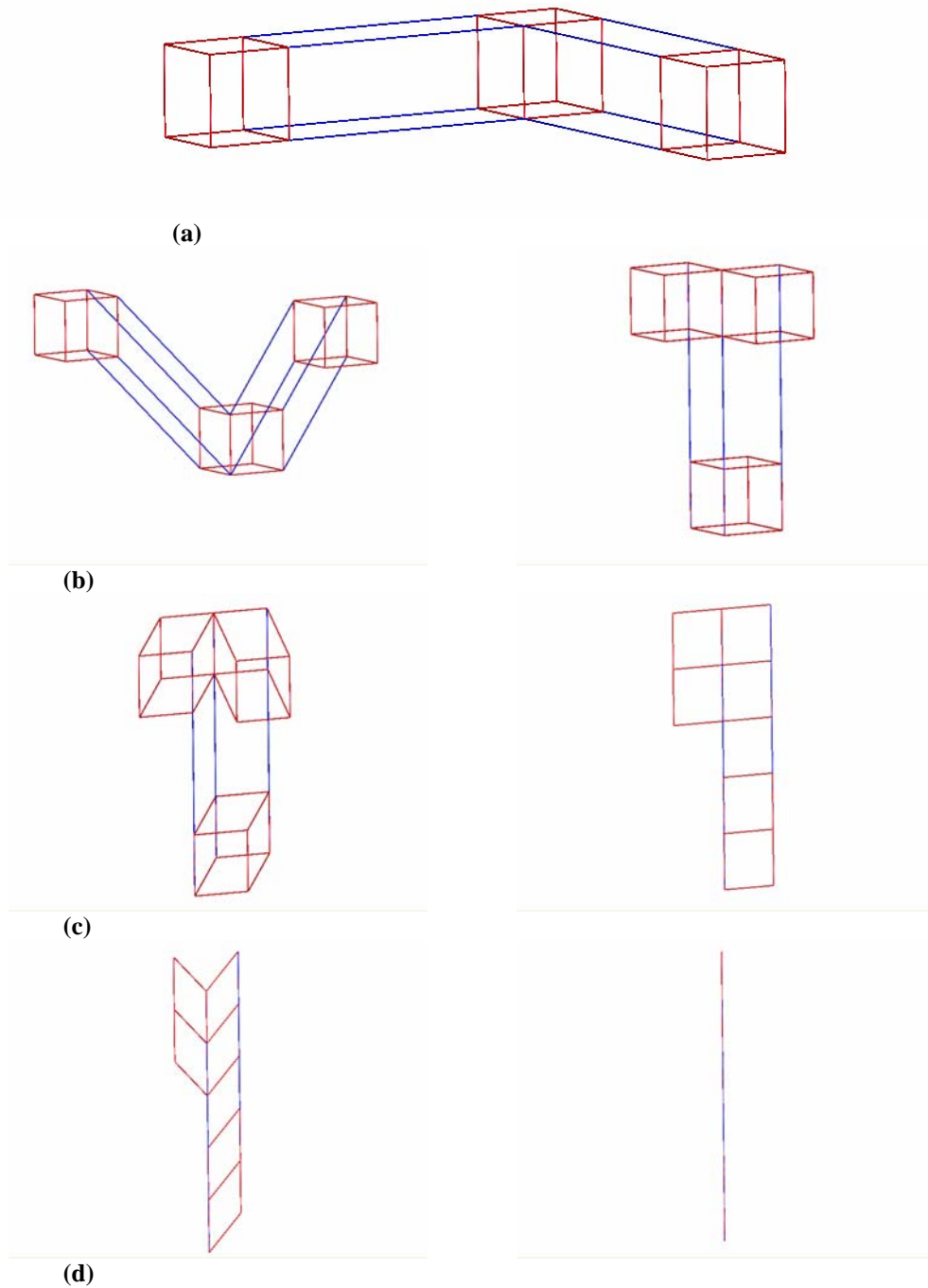


**Fig. 2** Example modeled assemblies of the truss concept depict the system at each stage of the deployment sequence, (a) two-, deployed trusses terminating at three-, deployed hub boxes; (b) simultaneously sheared truss bays to collapse these assemblies against faces of the hub boxes; (c) the first hub box shear and the second shear of the left truss as one event; (d) and the second hub box shear and the second shear of the right truss as one event.

## B. Background

Heritage deployable trusses package through a linear reduction in length while the diameter dimension remains relatively constant. Often, this form factor is not ideal for placement of the packaged truss in a launch fairing constrained by volume and other spacecraft components. There may be situations where a truss that packages through an increase in height in exchange for a greater reduction in length is more desirable. For example, the model depicted in Fig. 2 shows a truss that deploys radially outward from a bus yet utilizes more the extruded crescent shape volume formed between the bus and fairing wall without additional articulation being required. The boom achieves an extremely high compaction ratio by increasing the packaged height to decrease length.

## C. Objective

The objective of this research is to develop a novel, deployable hierarchical truss architecture composed of extruded CFRP rod and SMA flexure elements. The scope of this study encompasses applying fundamental principles of rational truss design, relevant to all deployable structures, first to prove the concept at the individual element level, then to design the packaging kinematics, and finally, evaluate and scale the global performance of the system.

## II. Individual Element Proof-of-Concept

The merit of the philosophy whereby individual elements are synthesized of structurally efficient material for the majority of their length and a less structurally efficient compliant material at either end of the span to permit articulation can be readily illustrated. The strength stability performance of the piece-wise constant cross-section element was compared against a conventional kinematic equivalent constant cross-section element (Fig. 3). The piece-wise element was supported with clamped boundary conditions, consistent with how this member would interface within the truss, and the conventional element was supported with pinned boundary conditions, as required to similarly articulate within the deployable truss. The critical, bifurcation load of the conventional element was determined analytically with the pinned-pinned Euler column buckling load formulation. The conventional element rod material properties and geometry were assumed as  $E_r=156$  GPa,  $d_r=1.27$  mm, and  $l_r=134$  mm, yielding 10.9 N.

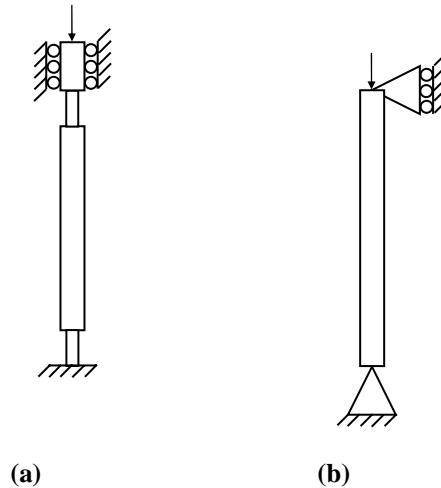


**Fig. 3 (a) Piece-wise constant cross-section element supported with clamped boundary conditions; (b) conventional kinematic equivalent constant cross-section element supported with pinned boundary conditions**

The critical load of the piece-wise element was predicted by employing the ABAQUS Standard finite element code's subspace eigensolver and representing the model with continuum elements.<sup>7</sup> The piece-wise element CFRP material properties were assumed to be identical to those of the conventional element rod and the SMA material properties were assumed as  $E_f=75.2$  GPa. The flexure geometry can partly be characterized by  $h_f=305$   $\mu$ m and  $b_f=1.47$  mm. The length of the flexures is driven by the allowable SMA strain at 5.00%, corresponding to the packaged configuration as well as other constraints arising from the joints design of the model to be discussed. The greatest flexure length,  $l_f$ , for the system considered is approximately 11.1 mm. In order to result in an equivalent

length element, the length of the piece-wise element rod section was reduced to 112 mm, for a total length of 134 mm. Interestingly, this ratio of stiffened center section length to the entire column length at 0.8 nears the optimal ratio found in Ref. 2 at 0.7. The first negative pivot for the piece-wise FE model occurs at 10.7 N (Fig. 4). Compromise of strength stability properties is unnecessary to substitute monolithic flexure hinged elements in place of traditional mechanically pinned joined truss members.

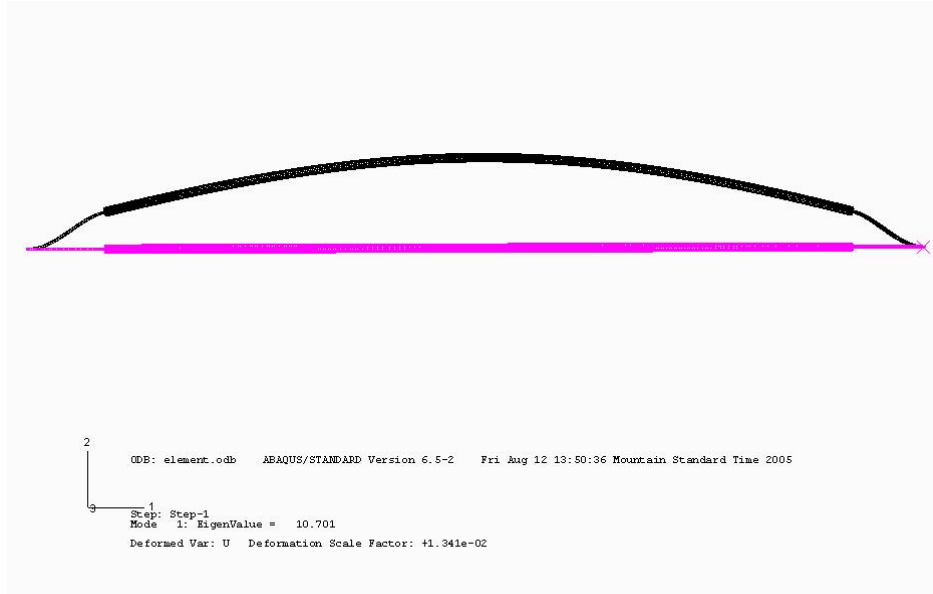


**Fig. 4 The first negative pivot for the piece-wise FE model occurs at 10.7 N.**

### III. Packaging Kinematics Design

The crux of the kinematics design illustrated in Fig. 2 is the engineering of the joints occurring at node locations throughout the truss network where they connect the CFRP and SMA elements as well as enforcing the flexure bend axis and radius. As anticipated to be first proto-typed these components were assumed to be composed of a photopolymer; a more structurally efficient material at these integral locations would pay dividends to global system performance. To appreciate the function of a joint, an individual monolithic joint is highlighted and tracked through the three packaging or deployment stages of two hub boxes and a single truss (Fig. 5). Notable features include wells for bonding both the CFRP rods and SMA flexures, radii contiguous between two joints to optimize nesting of a stowed hinge, and chamfer guides to enhance the determinability of the packaged state. Understandably, some intrinsic eccentricity will arise as truss elements due not coincidentally terminate at node points to purchase greater volume optimization of the stowed hinges. Ultimately, the outer radius of the joints is driven by the allowable SMA strain, again, 5.00% for the model considered.

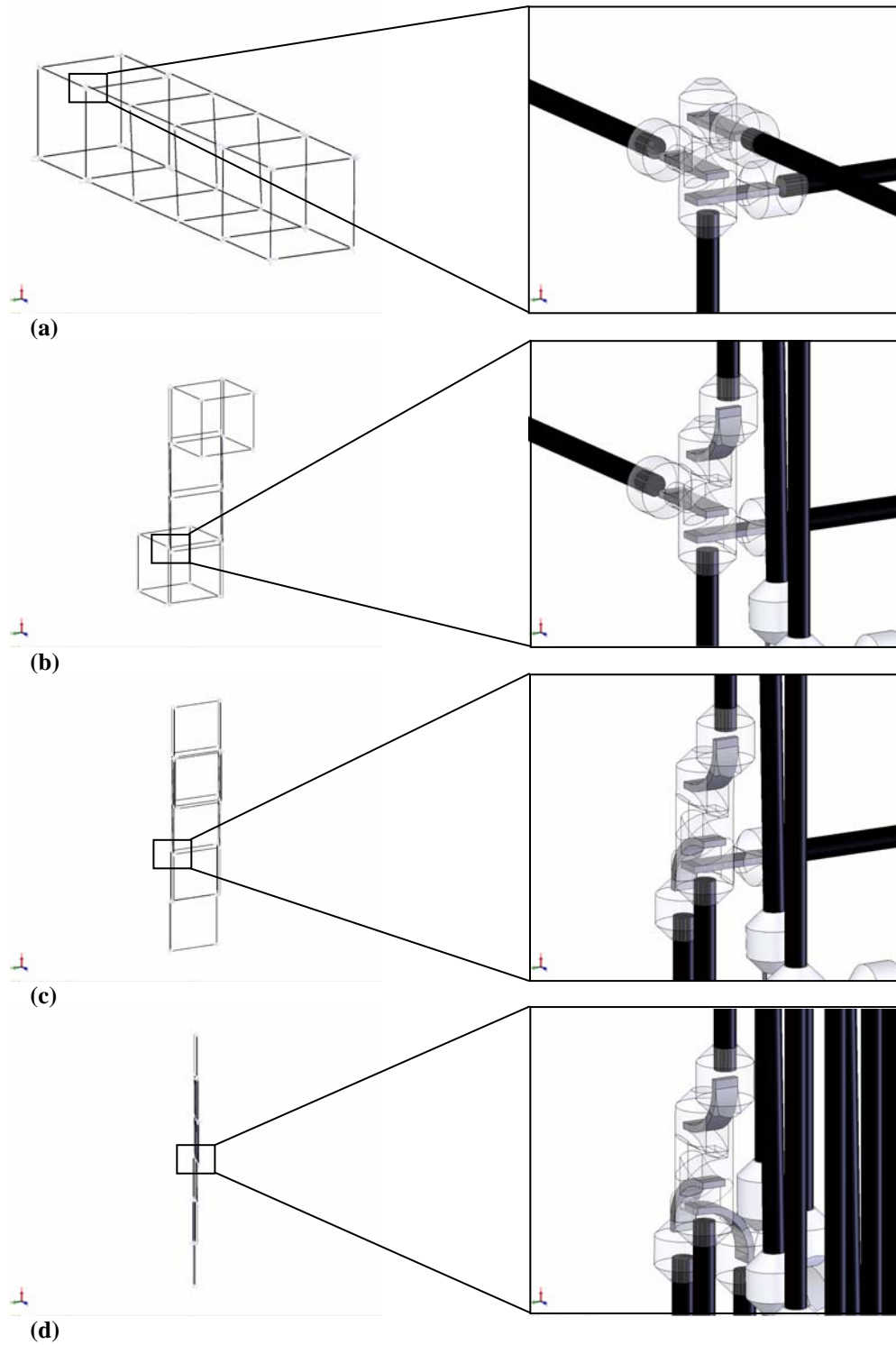


**Fig. 5** To appreciate the function of a joint, an individual monolithic joint is highlighted and tracked through the three packaging or deployment stages, (a) one-, deployed truss terminating at two-, deployed hub boxes; (b) simultaneously sheared truss bays to collapse this assembly against faces of the hub boxes; (c) the first hub box shear; (d) and the second hub box shear and the second shear of the truss as one event.

An additional dimension of the design space, temperature, exists attributable to the thermal-mechanical coupling of Nitinol's properties. For one engineering an SMA reinforced structure, material design must parallel the mechanical design to insure successful leverage of these features. Near eutectic NiTi micro-structure can only recover from detwinning, a deformation mechanism enabling inelastic strain limits measured between 8-9%;<sup>7, 8</sup> if the crystal lattice responds through twin boundary deformation along the martensite plane as a body centered tetrahedral, a less symmetric atomic ordering indicative of the low temperature phase or martensite.<sup>9, 10</sup> Thermoelastic phase transformation from the more ordered austenitic face centered cubic (FCC) micro-structure can be induced by an enthalpy rejection, motivation for the phenomenon commonly referred to as the shape memory effect (SME), a mechanical energy addition, or a combination of the two phenomena; tensile strain resulting from tractions and body loads also affects the transformation kinetics as a mechanical energy addition will result in stress induced martensite to a ceiling of approximately 50-80 K above the austenite finish temperature.<sup>11</sup> The engineering challenge is to spec an alloy which will be austenitic in the deployed service environment to exploit the higher performance FCC properties, but will not revert to austenite when subjected to integration and launch thermal-mechanical loads; if FCC retransformation occurs once strain packaged, the detwinning deviatoric mechanism may be exhausted and the SMA will respond to loads above the austenite proportional limit by slip or conventional plastic deformation. As a logistics example, the particular Nitinol alloy used for proto-typing has austenite finish and martensite start temperatures at approximately 260 K and 220 K, respectively. Once stowed, plastic deformation can be avoided by not exceeding 310-340 K and once deployed austenite properties can be expected by not ceding 220 K. To further exploit the thermo-mechanical nature of SMA for this architecture, the alloy can be tailored through deviations from the eutectic point of the nickel-titanium system and introduction of impurities to index the austenite start temperatures between the flexure sets participating in the three deployment stages,<sup>10</sup> i.e., to rely on solar heating rate to sequence the release of detwinning strain energy and, consequently, serve as a passive deployment event control authority.

#### IV. Evaluation and Scaling of Global System Performance

##### A. Truss

The piece-wise element model composed of an extruded CFRP rod and SMA flexure elements was extrapolated one-order greater in hierarchy to form a six-bay four-longeron truss junctioning at hub boxes (Fig. 6). This model geometry reflects the length of the element as each bay is approximately a 127 mm cube; recall the concept was conservatively studied at 134 mm to capture the longest CFRP and SMA span expected to occur in the truss-of-trusses network. Cross-sections of the piece-wise element components are identical to those considered for the proof-of-concept and proportioned according to the joints per Fig. 5. Constitutive properties were assumed to be  $E_f=75.2$  GPa,  $\nu_f=0.3$ ,  $E_p=2.76$  GPa, and  $\nu_p=0.34$  for the SMA and photopolymer, respectively, where as the orthotropic material constants of the CFRP were consistent with experimental results of the IM7/977-2 system;<sup>12</sup> the cross-section axial modulus of the diagonal elements communicating between joints across the bay faces was assumed at 507 N. Mass density properties followed  $\rho_r=1.63$  Mgm<sup>-3</sup>,  $\rho_f=6.45$  Mgm<sup>-3</sup>, and  $\rho_p=1.12$  Mgm<sup>-3</sup>; mass of the diagonal elements was not accounted for. This 29.1 g, 986 mm long structural model, assembled with tied constraints at rod-joint and flexure-joint interfaces to emulate a bonded, built-up prototype, is traceable to the second-order hierarchy element conceived to construct the one- and two-dimensional third-order hierarchy formats rendered in Fig. 1.

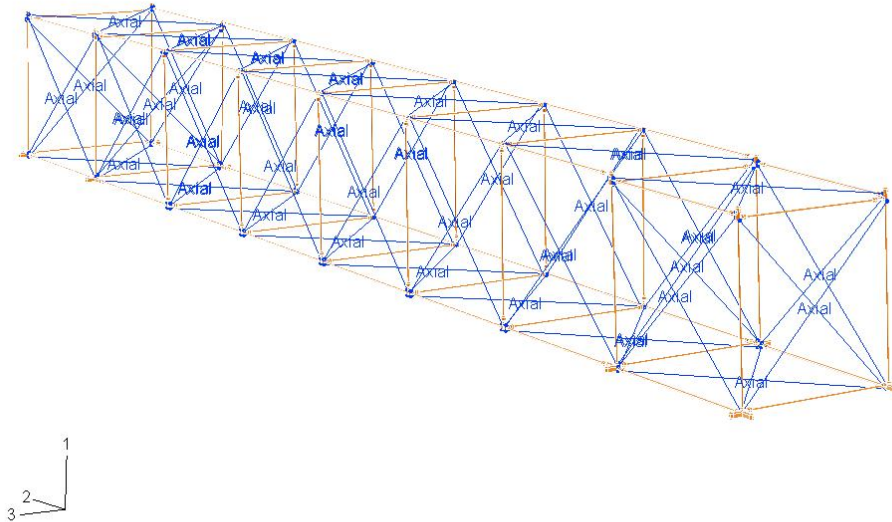


**Fig. 6** The piece-wise element model composed of an extruded CFRP rod and SMA flexure elements was extrapolated one-order greater in hierarchy to form a six-bay four-longeron truss junctioning at hub boxes.

This assembly with as mentioned geometry, material properties, and interactions represented by continuum elements was constrained at one-end with fixed boundary conditions for beam property identification, with respect to the coordinate system of Fig. 6, employing the ABAQUS Standard finite element code's static linear solver (Table 1). This one-dimensional representation, resulting from the reduction in dimensionality based on slenderness assumptions, enabled more efficient third-order hierarchy predictions.

**Table 1** This assembly with as mentioned geometry, material properties, and interactions represented by continuum elements was constrained at one-end with fixed boundary conditions for beam property identification, with respect to the coordinate system of Fig. 6, employing the ABAQUS Standard finite element code's static linear solver.

$EA$ , kN	$(EI)_{33}$ , $\text{Nm}^2$	$(EI)_{31}$ , $\text{Nm}^2$	$(EI)_{11}$ , $\text{Nm}^2$	$GA$ , kN	$GJ$ , $\text{Nm}^2$	$w$ , $\text{gm}^{-1}$
125	476	611	1,000	2.57	36.2	29.5

## B. Truss-of-Trusses

The representative beam model was finally extrapolated one-order greater in hierarchy to form a three-bay boom and a nine-bay grillage (Fig. 7). This model reflects both the geometry of the second-order truss as bays are 986 mm cubed and squared, respectively, and the properties as each element responds as Table 1. Third-order diagonal members were not incorporated; for kilometer-scale structures, bending mechanics are expected to dominate.

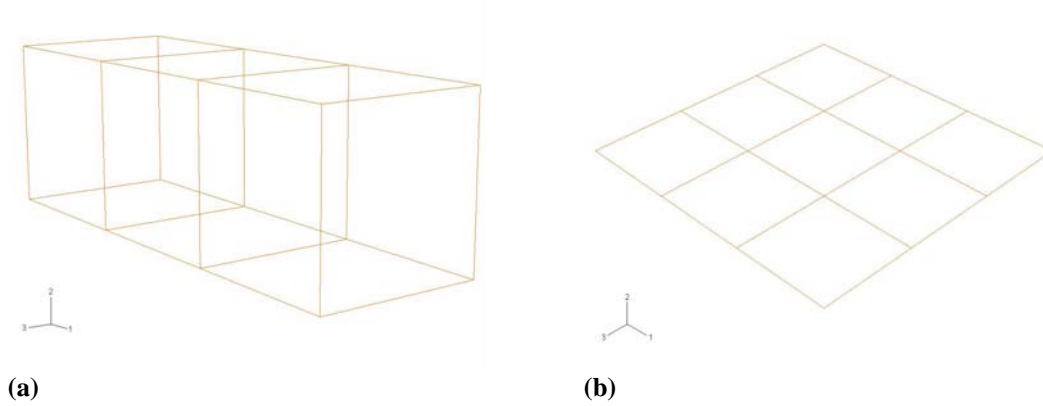


**Fig 7 The representative beam model was finally extrapolated one-order greater in hierarchy to form a, (a) three-bay boom; (b) and a nine-bay grillage.**

The third-order hierarchy formats were identified for both bending stiffness and bending strength-stability properties, with respect to the coordinate system of Fig. 7, in a similar approach to characterization of the second-order truss; the one-dimensional architecture was evaluated for cross-section bending moduli and corresponding critical moments and the two-dimensional architecture was evaluated for flexural rigidities and corresponding critical linear-moments (Tables 2, 3). A caveat regarding the reported critical moments: One should understand these reduced models do not have the resolution to perceive first-order hierarchy bifurcation modes.

**Table 2 Third-order hierarchy one-dimensional architecture was identified for cross-section bending moduli and corresponding critical moments, with respect to the coordinate system of Fig. 7, in a similar approach to characterization of the second-order truss.**

$(EI)_{33}$ , kNm <sup>2</sup>	$(EI)_{32}$ , kNm <sup>2</sup>	$(EI)_{22}$ , kNm <sup>2</sup>	$M_{33}$ , kNm	$M_{32}$ , kNm	$M_{22}$ , kNm	$w$ , gm <sup>-1</sup>
123	122	125	2.04	1.53	1.62	827

**Table 3 Third-order hierarchy two-dimensional architecture was identified for flexural rigidities and corresponding critical linear-moments, with respect to the coordinate system of Fig. 7, in a similar approach to characterization of the second-order truss.**

$D_{11}$ , kNm	$D_{13}$ , kNm	$D_{33}$ , kNm	$(MT^I)_{11}$ , N	$(MT^I)_{13}$ , N	$(MT^I)_{33}$ , N	$v$ , gm <sup>-2</sup>
74.6	166	74.6	162	188	162	79.9

With both third-order formats evaluated, global system performance implications of scaling the systems assumed at 20% structural mass fraction were investigated. Metrics traceable to mission requirements tracked include first free-free natural mode frequency and maximum tolerable angular acceleration, processing about mid-length.<sup>13</sup> The pacing properties assumed for the boom were  $(EI)_{32}$  and  $M_{32}$  (Fig. 8); the pacing properties assumed for the grillage were  $D_{11}$  and  $(MT^I)_{11}$  (Fig. 9).

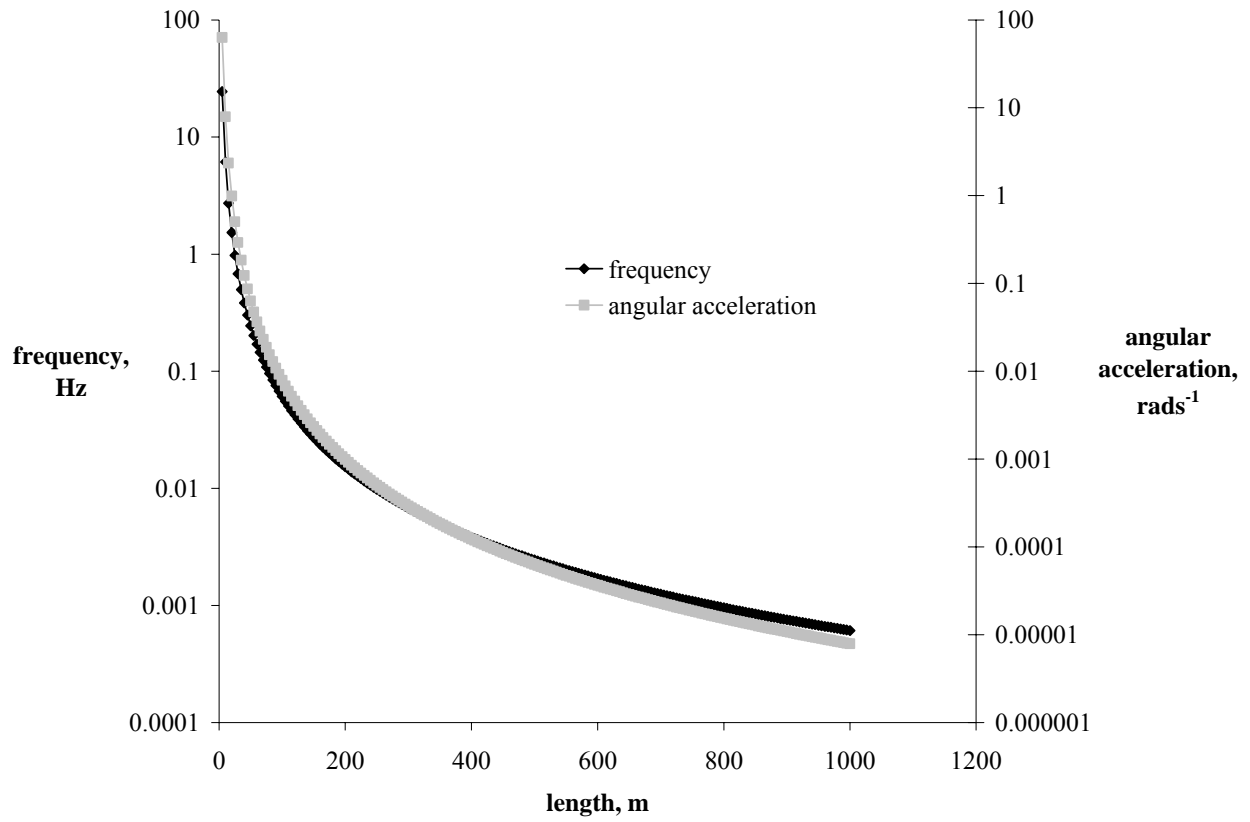


**Fig. 8 Metrics traceable to mission requirements tracked include first free-free natural mode frequency and maximum tolerable angular acceleration, processing about mid-length. The pacing properties assumed for the boom were  $(EI)_{32}$  and  $M_{32}$ .**

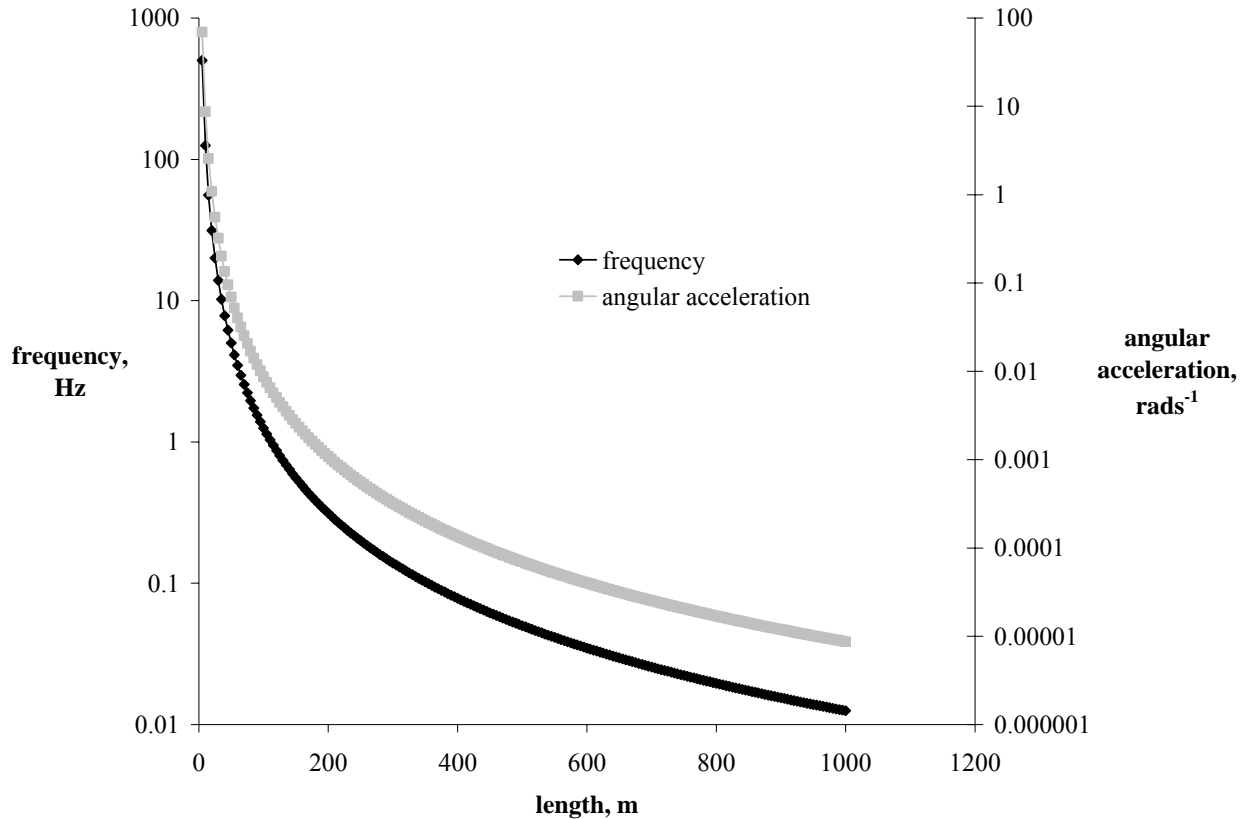


**Fig. 9 Metrics traceable to mission requirements tracked include first free-free natural mode frequency and maximum tolerable angular acceleration, processing about mid-length. The pacing properties assumed for the grillage were  $D_{11}$  and  $(MI^I)_{11}$ .**

## V. Conclusion

In review, research to develop a novel, deployable hierarchical truss architecture composed of extruded CFRP rod and SMA flexure elements has been documented; this structural system is representative of a concentrated, material deformation based deployable architecture. Linear compaction ratios of 400:1 and volumetric compaction ratios of 2,000:1 are reasonable. First, the concept at the individual element level was proven. Compromise of strength stability properties is unnecessary to substitute monolithic flexure hinged elements in place of traditional mechanically pinned joined truss members.

Then, the packaging kinematics were designed. The crux of the three-stage kinematics design is the engineering of the joints occurring at node locations throughout the truss network where they connect the CFRP and SMA elements as well as enforcing the flexure bend axis and radius. Ultimately, the outer radius of the joints is driven by the allowable SMA strain.

An additional dimension of the design space, temperature, exists attributable to the thermal-mechanical coupling of Nitinol's properties. The engineering challenge is to spec an alloy which will be austenitic in the deployed service environment to exploit the higher performance FCC properties, but will not revert to austenite when subjected to integration and launch thermal-mechanical loads; if FCC retransformation occurs once strain packaged the detwinning deviatoric mechanism may be exhausted and the SMA will respond to loads above the austenite proportional limit by slip or conventional plastic deformation.

Finally, the global performance of the system was evaluated and scaled. The piece-wise element model composed of an extruded CFRP rod and SMA flexure elements was extrapolated one-order greater in hierarchy to form a six-bay four-longeron truss junctioning at hub boxes. This assembly represented by continuum elements was

constrained at one-end with fixed boundary conditions for beam property identification. This one-dimensional representation, resulting from the reduction in dimensionality based on slenderness assumptions, enabled more efficient third-order hierarchy predictions. The representative beam model was extrapolated one-order greater in hierarchy to form a three-bay boom and a nine-bay grillage. Third-order diagonal members were not incorporated; for kilometer-scale structures, bending mechanics are expected to dominate. The third-order hierarchy formats were identified for both bending stiffness and bending strength-stability properties in a similar approach to characterization of the second-order truss. With both third-order formats evaluated, global system performance implications of scaling the systems were investigated. Metrics traceable to mission requirements tracked include first free-free natural mode frequency and maximum tolerable angular acceleration, processing about mid-length.

Fundamental principles of rational boom design relevant to all deployable structures have been applied to the truss-of-trusses architecture. Technology addressed through this research is intended to foster and mature successive large, launch-packaged concentrated strain structures.

### Acknowledgments

Support of this research is provided by the Air Force Research Laboratory Space Vehicles Directorate monitored by Dr. Jeffrey S Welsh.

### References

- <sup>1</sup>*Deployable Structures*, Edited by S Pellegrino, CISM Courses & Lectures, CISM, 2001.
- <sup>2</sup>Lake, MS & Mikulas, MM, "Analysis of a Simply Supported Column with a Piecewise Constant Cross Section," NASA Technical Paper 3090, 1991.
- <sup>3</sup>Birman, V, "Review of Mechanics of Shape Memory Alloy Structures," *Applied Mechanics Reviews*, Vol. 50, 1997, pp. 629-645.
- <sup>4</sup>*ABAQUS/Standard User's Manual*, Hibbitt, Karlsson, & Sorensen, Inc., 2004.
- <sup>5</sup>Von Roos, A & Hedgepeth, JM, "Design, Model Fabrication, & Analysis for a Four-Longeron, Synchronously Deployable, Double-Fold Beam Concept," Astro Aerospace Corp. AAC-TN-1139, 1985.
- <sup>6</sup>Hedgepeth, JM, "Pactruss Support Structure for Precision Segmented Reflectors," NASA CR-181747, 1989.
- <sup>7</sup>Mikulas, MM, Lou, MC, Withnell, PR, & Thorwald, G, "Deployable Concepts for Precision Segmented Reflectors," JPL D-10947, 1993.
- <sup>8</sup>Cross, WB, Kariotis, AH, & Stimler, FJ, "Nitinol Characterization Study," NASA CR-1433, 1970.
- <sup>9</sup>Proft, JL & Duerig, TW, "Mechanical Aspects of Constrained Recovery." *Engineering Aspects of Shape Memory Alloys*, Edited by TW Duerig, KN Melton, D Stockel, & CM Wayman, Butterworth-Heinemann, London, UK, 1990, pp. 115-129.
- <sup>10</sup>Tanaka, K, "Analysis of Recovery Stress and Cyclic Deformation in Shape Memory Alloys," *Advances in Continuum Mechanics*, Edited by O Bruller, Springer-Verlag, Berlin, D, 1991, pp. 441-451.
- <sup>11</sup>Funakubo, H, *Shape Memory Alloys*, Gordon and Bleach, New York, NY, 1987.
- <sup>12</sup>Xu, YB, Wang, RL, & Wang, ZG, "In-Situ Investigation of Stress-Induced Martensite Transformation in the Ni-Ti Shape Memory Alloy During Deformation," *Material Letters*, Vol. 24, 1995, pp. 355-358.
- <sup>13</sup>Welsh, JS & Wegner, PM, "The Effect of Adhesive Bond Thickness and Material Type on Structure Stiffness," *Proceedings of the 43rd AIAA/ASME/ASCE/AHS/ASC Structures, Structural Dynamics, and Materials Conference*, 2002-1726, AIAA, Washington, DC, 2002.
- <sup>14</sup>Blevins, RD, *Formulas for Natural Frequency and Mode Shape*, Van Nostrand Reinhold Company, 1979.